EVALUATION OF SCENE-BASED EMPIRICAL APPROACHES FOR ATMOSPHERIC CORRECTION OF HYPERSPECTRAL IMAGERY

A.H.Souri[1], M.A.Sharifi[2]

[1, 2] Department of Surveying and Geomatic Engineering, College of Engineering,
University of Tehran, Iran.
(souri_rs,sharifi)@ut.ac.ir

KEYWORDS: Remote sensing, atmospheric correction, hyperspectral, scene-based empirical

Abstract: The hyperspectral remotely sensed imagery is used in vast applications, especially in agriculture, mineralogy, geology, ecology and surveillance. Although it can give us abundant information with high spectral resolution, the presence of atmosphere with gases and aerosols alters the signal, leading to reduce and scatter the energy so that radiance does not interact with the ground surface. Therefore, if we demand reliable and accurate reflectance which is a property of ground feature, we have to carry out atmospheric correction for hyperspectral imagery. In this paper we evaluate scene-based empirical approaches that merely depend on statistics of image which can reduce the atmospheric effect without having any meteoric and geometric measurement. The results show that empirical line calibration is the most accurate method.

INTRODUCTION

Atmospheric constituents such as gases and aerosols have two types of effects on the radiance observed by a hyperspectral sensor:

- First it will result in the reduction of the energy that illuminates a ground of object (and being reflected from the object) at specific wavelengths.
- Second, the atmosphere acts as a reflector itself which will cause the addition of scattering, extraneous path radiance to the signal detected by the sensor which is irrelevant to the properties of the surface.

Although hyperspectral sensors are generally airborne, it's necessary to heed atmospheric effect in order to have reliable and accurate result.
Atmospheric correction techniques can be divided into two main categories including relative (empirical) and absolute (rigorous).Since 1985, atmospheric correction algorithms have promoted the empirical methods to rigorous modeling. (Bo-Cai Gao 2006)

Absolute atmospheric correction is more preferable than the relative correction techniques (Nikolakopoulos et. al., 2002) since it models the atmosphere according to the similar environmental and geographical conditions when the image is acquired however it definitely needs weather and meteoric measurements.

the Atmospheric CORrection Now (ACORN), the Fast Line-of-sight Atmospheric Analysis of Spectral Hypercubes (FLAASH), and ATmospheric CORrection (ATCOR 2-3) are now new approaches to reduce atmosphere effect by simplifying rigorous parameters to coefficients that depend on atmospheric and geometric conditions.

In this paper we introduce and evaluate empirical methods which merely rely on image data statistics and there is no need to know the signal wavelength, solar and viewing geometry and atmospheric parameters.

They are mainly five empirical techniques for correcting atmospheric effect:

1. Dark Object subtraction
2. Flat field calibration
3. IARR*
4. Log residuals
5. Empirical line calibration

* Internal Average Relative Reflectance

We utilize each of above techniques so that the resultant spectra can be compared with the reflectance spectra of the study area.

METHODOLOGY

As the recorded image data is digitized and rescaled to fit into 16 bit/pixel encoding, the correlation coefficient can subsequently be calculated between the calibrated radiance and reflectance.

In order to verify the efficiency of methods in different ground features, three locations (water, soil and vegetation) have been selected.

The spectral correlation measure (Van der Meer and Bakker, 1997) is calculated as the correlation coefficient of the pixel (portrayed as vector in a n-dimensional feature space) $r_i = (r_{i1}, ..., r_{iL})^T$ and $r_j = (r_{j1}, ..., r_{jL})^T$ and their respective reflectance $s_i = (s_{i1}, ..., s_{iL})^T$ and $s_j = (s_{j1}, ..., s_{jL})^T$ as:

$$r_{si,sj} = \frac{n\sum_1^n s_i s_j - \sum_1^n s_i \sum_1^n s_j}{\sqrt{\left[n\sum_1^n s_i^2 - \left(\sum_1^n s_i\right)^2\right]\left[n\sum_1^n s_j^2 - \left(\sum_1^n s_j\right)^2\right]}} \quad (1)$$

where n is number of the overlapped band.

The correlation coefficient has advantage that it takes into account the relative shape of radiance curve as well as reflectance curve. (Freek van der Meer 2005)

Each algorithm will be outlined in more detail in what follows.

Dark object subtraction

The most significant radiation components seen at the sensor are generally unscattered and down-scattered surface-reflected, and path-scattered (Schowengerdt, 1997). A usual simplification is to assume that down-scattered atmospheric radiance is zero.

Features like water and asphalt can be regarded as dark objects. We assume the dark objects reflect no light, any value greater than zero must result from atmospheric scattering. We remove this scattering by subtracting the lowest brightness value (dark object) from every pixel in the band.

Flat field calibration

Flat Field calibration produces relative reflectance by dividing the mean spectrum of a user-defined region of interest (ROI) into the spectrum of each pixel in the image. The ROI should be a spectrally flat material within the wavelength range of the sensor. Beach sand and concrete are popular choices and vegetation is poor choices.

IARR

IARR algorithm is similar to Flat Field calibration in that a reference spectrum is divided into each pixel in the image to generate relative reflectance. However, the reflectance spectrum for IARR is the mean spectrum of the entire image versus a user-defined ROI.

Two above methods assume that the flat area should have neutral spectrum and any deformation of signal could be generated by atmosphere so dividing the mean spectrum into each pixel can reduce this error in the whole image.

Log residuals

The Log Residuals method produces a pseudo reflectance dataset by dividing each pixel's spectrum by the spectral geometric mean and the spatial geometric mean.

Normalization is an alternative which makes the corrected data independent of multiplicative noise such as topographic and illumination factor effects which depend on atmosphere parameters. This can be performed using Log Residuals, based on the relationship between radiance and reflectance:

$$X_{i,n} = T_i R_{in} I_n,\ i = 1,\ldots,K;\ n = 1,\ldots,N \quad (2)$$

Where $X_{i,n}$ is radiance for pixel i in wavelength n. T_i is the topographic effect, which is assumed constant for all wavelengths. R_{in} is the real reflectance for pixel i in wavelength band n. I_n is the (unknown) illumination factor, which is assumed independent of pixel. K and N are the total number of the pixels in the image and the total number of bands, respectively.

$X_{i,n}$ can be made independent of T_i and I_n by dividing $X_{i,n}$ by its geometric mean over all bands and then its geometric mean over all pixels. The result is not identical to reflectance but is independent of the multiplicative illumination and topographic effects present in the raw data. The procedure is carried out logarithmically so that the geometric means are replaced by arithmetic means and the final result obtained for the normalized data is:

$$LogZ_{i,n} = logX_{i,n} - (\frac{1}{N}) \sum_{n=1}^{N} logX_{i,n} - (\frac{1}{K}) \sum_{i=1}^{K} logX_{i,n} \quad (3)$$

Empirical Line Calibration

Empirical Line calibration forces the image spectra to match reflectance spectra collected from the field. This method can produce the most accurate results possible, but it requires ground truth information.

A simplified view is that remote measurements have lost DN_k and/or accumulated unwanted DN_k in each wavelength channel owing to several possible processes. The effects of some processes are multiplicative, others are additive. (John B.Adams , Alan R.Gillespie 2006)

$$DN_k = G_k \times L_k + O_k \quad (4)$$

K is number of band, L_k is the measured value of a pixel in band k; DN_k is the corrected value of a pixel in band k; O is offset and G is gain in band k.

In this method the gain and offset will be calculated for selected locations in each of channels, then we exert Offset and Gain coefficient on all pixels for each of channels:

$$DN_k = \left(\frac{1}{G_k}\right) \times (L_k - O_k) \quad (5)$$

STUDY AREA AND USED DATA

The study area is ProSpecTIR-VS image located on Reno, NV, USA that's retrieved from SpecTIR Company.The ProSpecTIR-VS instrument has dual sensors individually covering visible/near-infrared (VNIR) wavelengths of 400-1000nm and short-wave infrared (SWIR) in the 1000-2500nm wavelength range within 360 channels and 2m spatial resolution.

The image located in Reno is covered by urban and mixed environment (Fig1). In order to perform appropriate comparisons of the atmospherically corrected images, three sample locations are selected: Vegetation, Soil and Water.

Fig.1. Reno, NV, USA

The location has two individually reflectance and radiance images so that evaluation of signal deformation could be possible.

RESULTS AND DISCUSSION

In order to evaluate the capability of methods, three reflectance and radiance such as soil, vegetation and water have been selected in study area.

The radiance and reflectance curve of above locations are indicated in Figure 2, 3.

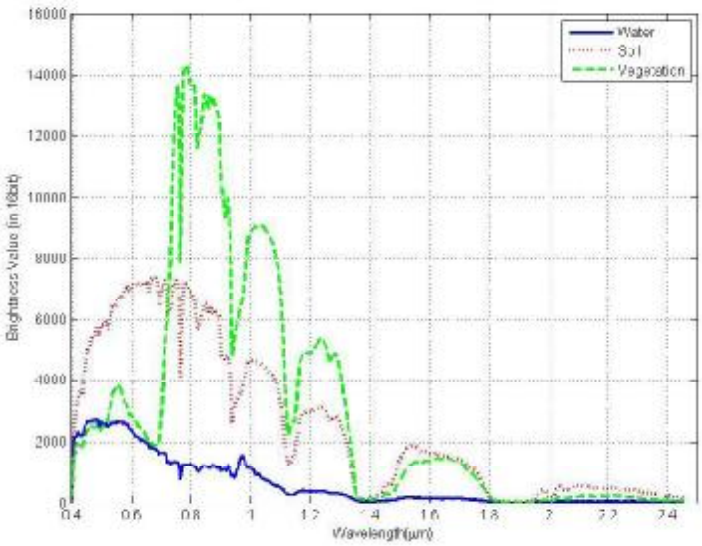

Fig.2. Radiance curve of selected area

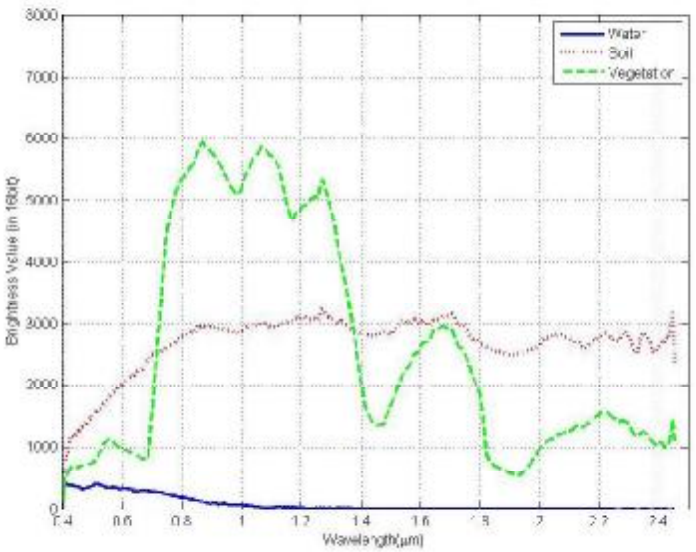

Fig.3. Reflectance curve of selected area

There were no clouds and aerosols seriously when image was acquired so merely slight difference between radiance and reflectance could be distinguished in visible light (0.4 to 0.7μm). But in presence of water vapor and gases, the difference will dramatically increase in subsequent bands.

According to figure 4 the main absorbing gases in the atmosphere are water vapor, ozone, carbon dioxide, and oxygen. Atmospheric water vapor focused at 0.94, 1.14, 1.38 and 1.88 μm, the oxygen gas at 0.76 μm, and the carbon dioxide near 2.08 μm .We can conclude that approximately more than half of the spectral region is affected by atmospheric gas absorptions. The shorter wavelength region below 1 μm is also affected by molecular and aerosol scattering. (Bo-Cai Gao 2006)

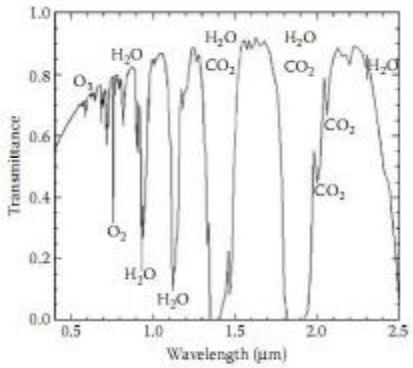

Fig.4. Atmospheric transmittance in the 0.4μm to 2.5μm

The spectrum profile of calibrated radiance and the reflectance in flat region are shown in figure 5, 6 respectively.

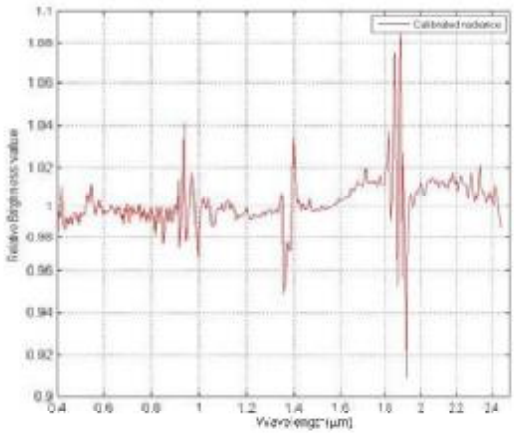

Fig.5. Calibrated radiance of flat region by flat field method

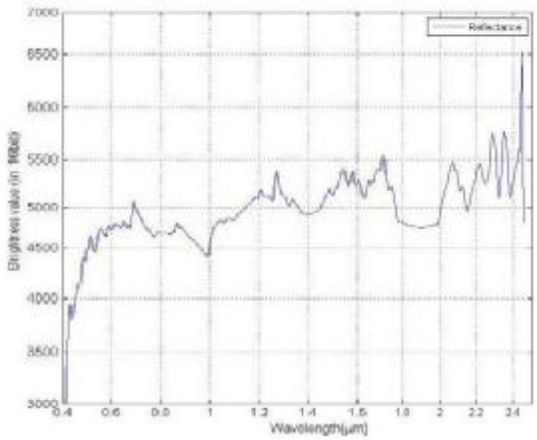

Fig.6. Reflectance of a flat region

The result of Log residuals method is shown in Fig 7. The relative brightness value in log residuals demonstrates the value of absorption in all bands, for instance white feature in RGB image absorbed approximately all of the energy in all bands. This concurs well with our knowledge that water is almost a black object. For illustrating more clearly, vegetation intensely emits energy in more than half of channels in relative of other features; so we expect the vegetation appears black.

Fig.7. Log residuals result in RGB bands.

To compare the comparability between the calibrated radiance corrected by the methods and the reflectance curves, we compute the correlation coefficient (see table 1).

Table 1. correlation coefficient between calibrated radiance and reflectance

	Water	Soil	Vegetation
primary radiance	0.9492	0.3497	0.7922
Dark object subtraction	0.9053	0.2422	0.3760
Flat field calibration	0.2276	0.8225	0.9620
IARR	0.4797	0.7103	0.9766
Log residuals	0.5252	0.6308	0.9797
Empirical line calibration	0.8789	0.9421	0.9911

CONCLUSIONS

1. Dark object subtraction method can damage seriously the image unless it's being used for visible range. In other word this simple technique is effective for haze correction in multispectral data in the shorter wavelengths where scattering dominates, however it should not be used for hyperspectral data
2. Flat field calibration and IARR are effective in soil and especially vegetation but it also could damage image in 1, 1.36 and 1.8μm (see Fig5, 6) where water vapor changes the spectra approximately. These methods assume that flat ROI has spectrally neutral and the relative spectra often have absorption features that are not present in reflectance spectra of comparable materials measured in the field or laboratory. (Bo-Cai Gao 2006)
3. Log residuals can be useful for vegetation analysis but it's usually more effective for analyzing absorption features present in hyperspectral data rather than removing atmospheric effect.
4. If the flat area is available in location, flat field calibration and IARR can be effective in removing atmospheric effect in vegetation analysis.
5. The presence of water vapor is the main reason in hyperspectral imagery that hinders the empirical methods to operating more effectively.

6. Empirical line calibration is the most accurate and effective method in scene-based empirical methods but it needs field or laboratory information.

REFERENCES

1. John,A.Richards,Xiuping,Jia, 2006, Remote Sensing Digital Image Analysis, Australia, Springer-Verlag Berlin Heidelberg.
2. Qihao, Weng, 2011, Advances in Environmental Remote Sensing Sensors, Algorithms, and Applications, Taylor & Francis Series, Indiana state University.
3. John, B.Adams, Alan, R.Gillespie,2006, Remote Sensing of Landscapes with Spectral Images, Cambridge University,
4. B.Ramachandra, Christopher, O.Justice, M.J, Abrams,2011, Land Remote Sensing and Global Environmental Change,NASA publications.
5. Xia Zhang,Hang Yang,Tong Shuai, 2004, Comparison of FLAASH versus Empirical Line Approach for AtmosphericCorrection of OMIS-II Imagery, Chinese Academy of Sciences, Beijing.
6. E., Karpouzli, T., Malthus, 2003. The empirical line method for the atmospheric correction of IKONOS imagery,Int.J.Remote Sensing,Vol. 24, No. 5, pp. 1143-1150.
7. Chavez, P. S., 1996, Image-based atmospheric corrections revisited and improved.Photogrammetric Engineering and Remote Sensing, 62, pp. 1025–1036.
8. Gordon, H. R.,1997, Atmospheric correction of ocean colour imagery in the Earth Observing System era. Journal of Geophysical Research-Atmospheres, 102, 17 081–17 106.
9. Farrand.W.H., Singer.R.B., E. Merenyi, 1994, Retrival of Apparent Surface Reflectance from AVIRIS Data: A Comparision of Empirical Line, Radiative Transfer, and Spectral Mixture Mothods. Remote Sensing of Environment, 47: pp. 311-321.
10. B.,T.,San ,M.,L.,Suzen , 2010, evaluation of different atmospheric correction algorithms for eo-1 hyperion imagery , International Archives of the Photogrammetry, Remote Sensing and Spatial Information Science, Volume XXXVIII, Part 8, Kyoto Japan.
11. Nikolakopoulos, K.G.,Vaiopoulos, D.A., Skianis, G.A.,2002, A Comparative Study of Different Atmospheric Correction Algorithms Over An Area With Complex Geomorphology in Western Peloponnese, Greece, Geoscience and Remote Sensing Symposium, IGARSS '02, IEEE International, 4, pp. 2492 – 2494.
12. Bo-Cai,Gao,Curtiss,O. Davis,Alexander F. H. Goetz, 2010, A Review of Atmospheric Correction Techniques for Hyperspectral Remote Sensing of Land Surfaces and Ocean Color,IEEE.
13. Abramson, S. and Schowengerdt, R.,1993, Evaluation of edge-preserving smoothing filters for digital image processing, ISPRS Journal of Photogrammetry and Remote Sensing, 48:2-17.
14. Teillet, P., Fedosejevs, 1995, on the dark target approach to atmospheric correction of remotely sensed data", Canadian Journal of Remote Sensing, 21: pp.374-387.
15. Roberts, D.A., Yamaguchi, Y.,1985 and Lyon, R.J.P., Calibration of Airborne Imaging Spectrometer Data to percent Reflectance Using Field Spectral Measurements, 19 the International Symposium on Remote Sensing of Environment, Ann Arbor, Michigan.